

Tuning the Performance of Layer-by-Layer Assembled Organic Light Emitting Diodes by Controlling the Position of Isolating Clay Barrier Sheets

Michel Eckle[†] and Gero Decher^{*,†,‡}

Centre National de la Recherche Scientifique (CNRS), Institut Charles Sadron, 6 rue Boussingault, F-67083 Strasbourg-Cedex, France, and Université Louis Pasteur (ULP), 1 rue Blaise Pascal, F-67008 Strasbourg-Cedex, France

Received October 16, 2000

ABSTRACT

We have fabricated organic light emitting diodes (OLEDs) based on poly(*p*-phenylenevinylene) (PPV) and poly(methacrylic acid) (PMA), including an isolating layer composed of montmorillonite. We show that the single clay layer influences the behavior of the devices, lowering current densities and increasing light output in comparison with pure polymer systems. The subnanometer positioning of this isolating barrier within the active medium with respect to both electrodes, which is easily controlled by the deposition sequence, plays a key role for the electrooptical properties of the diodes.

In this report, we show a new method of controlling the architecture of polymeric LEDs^{1–3} composed of the classic PPV. The layer-by-layer technique^{4,5} used to fabricate devices offers the advantages of being solution based, allowing facile variation of film architecture (layer sequence), and effortless integration of many different materials such as polyelectrolytes, colloids, proteins, or inorganic charged species, most of them used for non-LED applications, but also for engineering LED interfaces.³ The basic OLED architecture of our choice is the LED described and optimized by Rubner et al.,^{6,7} based on 20 layer-pairs of PPV and PMA. Hybrid organic and nanoparticle-based systems have been recently studied as prospective materials for optoelectronic applications because they combine the advantages of organic polymers with those of inorganic clusters.^{8–13}

Hybrid films of polyelectrolytes and montmorillonite platelets are easy to fabricate and have been reported on before.^{14–18} The latter multilayers are similar in structure to the so-called polymer-layered silicate nanocomposites^{19,20} or pillared intercalates,^{21,22} which are interesting materials themselves.

The work reported here is an example of positioning an isolating layer of montmorillonite with subnanometer precision in the active part of a OLED of about 83 nm thickness only. In a multilayer OLED composed of 20 layers of PPV, one can place the isolating layer at each of the 19 positions

between PPV layers. This was done by maintaining exactly the thickness of the device and thus the amount of active material. Our intention to use a thin film of an isolating inorganic material (the thickness of the clay platelets is approximately 1 nm) was to modify the transport properties of electrons and holes through the active zone in a very controlled way. The inorganic barrier layer alters the transport properties of the semiconducting PPV although the effect may be explained in different ways. One could expect accumulation of space charges above and below the montmorillonite layer or, since the layer is composed of individual clay sheets, that charge transport proceeds predominantly through defects between platelets. Both models should lead to enhanced recombination efficiency (see also Figure 7). Since recombination is expected to be favored in the vicinity of the isolating layer, the layer-by-layer deposition technique could offer a low cost but highly precise way to shift the recombination zone through an OLED and to tune device performance. We are aware that the direct determination of the emission zone is not trivial²³ and we do not attempt to verify the position of the recombination zone in our devices in this first report. In the present work we have exemplarily chosen positions 2, 10, and 19 to show the principle effects of an isolating layer in LEDs. Precision placement of layers of different materials in organic multilayer LEDs can be very difficult using existing techniques.

The dimension of the light emitting area of our samples is typically 20 × 15 mm, which is otherwise not easily

[†] Institut Charles Sadron.

[‡] Université Louis Pasteur.

realized in nonspecialized laboratories. The large size of our samples also serves the purpose of showing that layer-by-layer assembly yields electroluminescent films that are homogeneous over large areas even without taking special precautions. It should be mentioned that all LEDs were fabricated in regular chemistry labs and not under clean room conditions.

Poly(ethylenimine) (PEI), $M_w \approx 50,000$, and PMA, $M_w \approx 9,500$, were purchased from Aldrich. The cationic precursor polyelectrolyte (pre-PPV) of the conjugated semiconducting polymer PPV was synthesized using the method described by Wessling²⁴ and Lenz.^{25,26} Pre-PPV was separated from residual monomer and NaOH by extensive dialysis against deionized water for 4 days (lower-limit molecular weight cutoff of 10 000). Because of the difference between batches of pre-PPV synthesized at different times or in different laboratories, we have reevaluated the optimum deposition and processing conditions (pH, salt concentration, elimination temperature). Pre-PPV was deposited from 3.0×10^{-2} monomolar solution (0.3 M NaCl, pH adjusted to 4.5 with HCl). Thermal conversion from pre-PPV to PPV was carried out at 270 °C for 12 h under vacuum. PEI was deposited from 2.9×10^{-2} monomolar solution, PMA, 3.0×10^{-3} monomolar solution (pH adjusted to 3.5 using HCl). Monomolar refers to one repeat unit of the polymer chain. Montmorillonite (Mont) was dispersed by ultrasonification in pure water until the solution appears clear. Suspensions with a concentration of dry montmorillonite of 7.5 mg/100 mL were used for the deposition of the montmorillonite layer.

The ultrapure water used for all experiments and for all cleaning steps was obtained by reversed osmosis (Milli-RO 35 TS; Millipore GmbH) followed by ion exchange and filtration steps (Milli-Q, Millipore GmbH). The resistivity was better than 18 MΩ cm and the total organic content less than 10 ppb (according to manufacturer).

The silicon slides used for ellipsometric thickness measurements were cleaned by a 1 h immersion in a 1:1 mixture of methanol and hydrochloric acid, followed by an extensive rinse with Milli-Q water and a second immersion in concentrated sulfuric acid for at least 1 h and a further rinse with Milli-Q water.


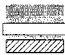


The ITO-coated glass substrates (Balzers GmbH, Germany), were patterned by etching a part of ITO with hydrochloric acid. Consecutive cleaning was achieved by heating the substrates in a 5:1:1 mixture of H₂O, H₂O₂ and NH₃,²⁷ following an extensive rinse with Milli-Q water.

The cleaned substrates were then functionalized by adsorption of a single layer of PEI.

Samples were made on Si-wafers and on ITO slides in parallel using an automated deposition device (Riegler & Kirstein GmbH, Suarezstr. 28, D-14057 Berlin, Germany). Both types of support were dipped at the same time into identical solutions in order to ensure the deposition of essentially identical films on the two different substrates.

Multilayers of pre-PPV and PMA were prepared by a cyclic immersion of the PEI coated substrates in pre-PPV and PMA solutions with 3 intermediate washing steps. The adsorption time was typically 20 min for pre-PPV and PMA.

Table 1. Deposition Sequence and Film Architecture of the Four Types of Multilayer Films Used in This Study^a

sample ID	OLED architecture	graphic representation
MLA-1	ITO/PEI/PMA/(PPV/PMA) ₂₀ /Al	
MLA-2	ITO/PEI/PMA/(PPV/PMA)/(PPV/Mont)/(PPV/PMA) ₁₈ /Al	
MLA-3	ITO/PEI/PMA/(PPV/PMA) ₉ /(PPV/Mont)/(PPV/PMA) ₁₀ /Al	
MLA-4	ITO/PEI/PMA/(PPV/PMA) ₁₈ /(PPV/Mont)/(PPV/PMA)/Al	

^a MLA-1 contains no clay layer, MLA-2 contains a single clay layer at position 2 (after the second PPV layer), MLA-3 contains a single clay layer at position 10, and MLA-4 contains a single clay layer at position 19. All multilayer samples contain a total of 20 PPV layers. With the exception of the montmorillonite layer, all other counterion layers are composed of poly(methacrylic acid) (PMA). The thicknesses of the active layer (gray) and the isolating layer (white box) on the substrate (hatched box) are not to scale for better readability.


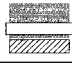


During the 3 washing steps the substrate is immersed and withdrawn 20 times for 5 s in the first beaker, 5 times for 20 s in the second beaker, and once for 60 s in the third beaker. Immersion/withdrawing cycles compensate for not stirring the solutions, three beakers are used in order to minimize cross-contamination by liquid adhering to the samples. The adsorption time for the montmorillonite layer was 15 min followed by 3 washing steps as described before. The individual samples are described in the text.

Ellipsometric measurements were performed using a wavelength of 632.8 nm (He–Ne laser) at an angle of 45° (Plasmos SD2300). They represent an average of 10 different points after deposition of a given number of layers. UV/vis spectra were taken at a Shimadzu UV-2101PC spectrophotometer. Light emission was detected in forward bias by using a silicon detector 71882 from Oriel Instruments with a typical responsivity of 4×10^8 V/Watt. In the figures we give the raw data in volts, obtained at a distance of OLED and detector of 1 cm. Emission spectra were recorded on a Hitachi F-4010 fluorescence spectrophotometer.

OLED Architectures. The electroluminescent behavior of OLEDs composed of 20 layer-pairs of PPV and PMA (ITO/PEI/PMA/(PPV/PMA)₂₀/Al) has been reported before,^{6,7} and this well established system was used as the basis for the modifications of the film architecture reported here. Since we have synthesized the precursor polymer of PPV ourselves, we have used slightly different fabrication conditions for our OLEDs as the ones reported by Rubner et al. before.^{6,7} The architecture of the different OLED devices is shown in Table 1.

The thicknesses of these samples (Table 2) have been measured by ellipsometry on Si wafers before thermal conversion after being conserved 24 h under vacuum (0.1 mbar) to remove water, and finally, after thermal conversion at 270 °C for 12 h under vacuum (0.1 mbar).

Table 2. Thickness of the Films on Si Wafers Measured before and after Thermal Conversion by Ellipsometry

Samples	Thickness before thermal conversion (Å)	Thickness after thermal conversion (Å)	Shrinkage percentage (%)
	1187	836	29.6
	1192	826	30.7
	1195	827	30.7
	1200	825	31.2

Optical Device Characteristics. UV/vis spectra (Figure 1) were taken after the thermal conversion of the respective OLED devices on ITO-coated glass, before the coverage with the aluminum cathode under vacuum (10^{-5} mbar).

We observe that the absorbance at the maximum of 412 nm is almost identical for films including a montmorillonite layer at different positions and those without, indicating that all samples contain the same amount of conjugated PPV. This also indicates that there are no major orientation or interfacial effects induced by the clay layer. Even in samples composed of several montmorillonite layers, the spectral characteristics do not change (data not shown, samples not discussed in this work).

After characterization of the films, the aluminum electrode was vapor deposited on the top of the films and optoelectronic characteristics were measured in forward bias. There were no special precautions taken to stabilize the LEDs or to prolong its lifetime.

Electrical Device Characteristics. The current–voltage profiles of our samples are given in Figure 2. The device

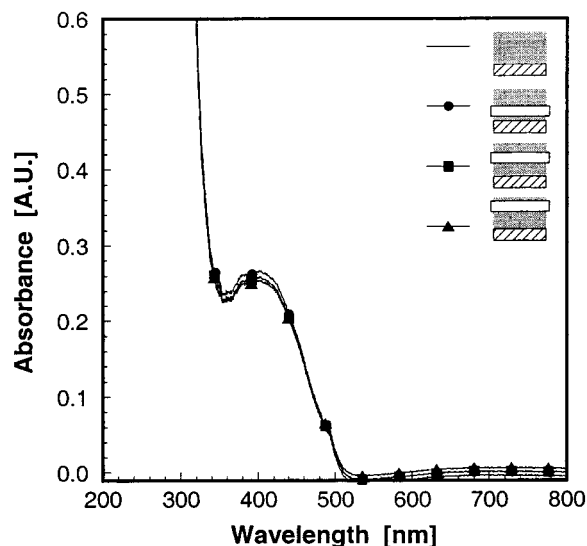


Figure 1. Absorbance spectra measured on ITO after thermal conversion, before evaporation of the aluminum electrode. The peak at 412 nm corresponds to the absorbance maximum of PPV. All samples show almost identical spectra, indicating that the amount of PPV in each LED is constant. Only a few data points are marked with symbols.

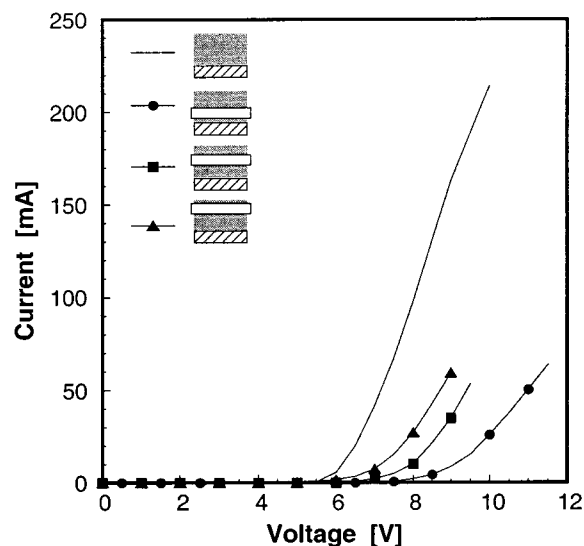


Figure 2. Current–voltage profiles of films of the four different architectures. Symbols represent a few experimental values only. When an isolating clay layer is introduced in the active media of the OLED, the turn-on voltage of the device is increased. Therefore, MLA-1 (straight line) has a higher turn-on voltage than MLA-2 (filled circles), MLA-3 (filled squares), and MLA-4 (filled triangles). When the clay layer is close to the ITO anode, the threshold voltage is highest.

without montmorillonite has a turn-on voltage of about 6 V, whereas the systems containing the isolating layer show a slightly higher turn-on voltage of 6.5–8.5 V.

By normalizing the current with the active area, and the voltage with the thickness of the individual samples, we can draw the current density versus the apparent macroscopic applied electrical field (Figure 3). LEDs containing an isolating layer need a higher threshold electrical field than those without. We also see that the position of the montmorillonite layer plays a key role in the value of the turn-on electrical field: when the inorganic layer is positioned close to the metallic cathode (MLA-4), the threshold value of the electrical field is lower in comparison with the case where the isolating layer is close to the ITO anode (MLA-2).

Electrooptical Device Characteristics. The light output from the LEDs has been measured and plotted versus the electrical field (Figure 4). In contrast to Figure 3, where the onset of current increase is observed at different electric fields, light starts being emitted at 0.6 MV/cm in all 4 OLED architectures. This already shows that less current is needed for light emission in the case of montmorillonite containing sample.

The curves of luminescence versus current density are even more interesting (Figure 5). The slope of these curves gives an idea of the relative efficiency of the devices. We immediately see that the introduction of a single layer of montmorillonite greatly enhances device performance. Furthermore, when the distance between the clay layer and the ITO anode increases, the efficiency becomes slightly smaller.

Emission Spectra. The emission spectra shown in Figure 6 clearly demonstrate that samples with or without a montmorillonite layer emit light of identical spectral com-

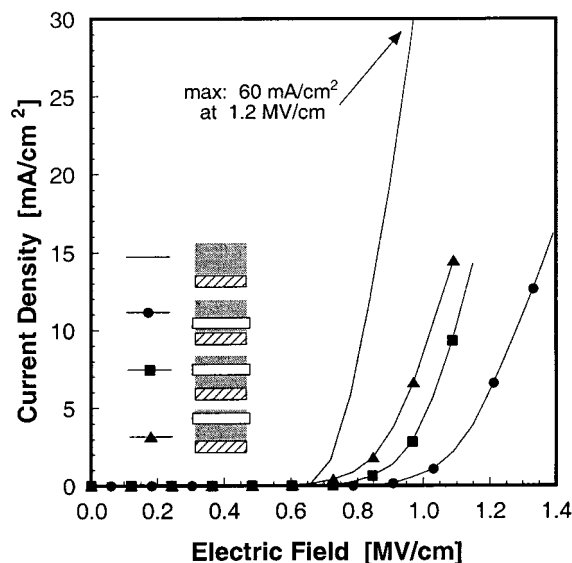


Figure 3. Current density vs electric field curves obtained from normalization of current with light emitting area and voltage with film thickness. MLA-1 (device without clay layer, straight line) has a lower turn-on electric field than devices with an isolating layer. As before (Figure 2), the threshold electric field is highest when the position of the montmorillonite layer is close to the ITO anode (MLA-2, filled circles).

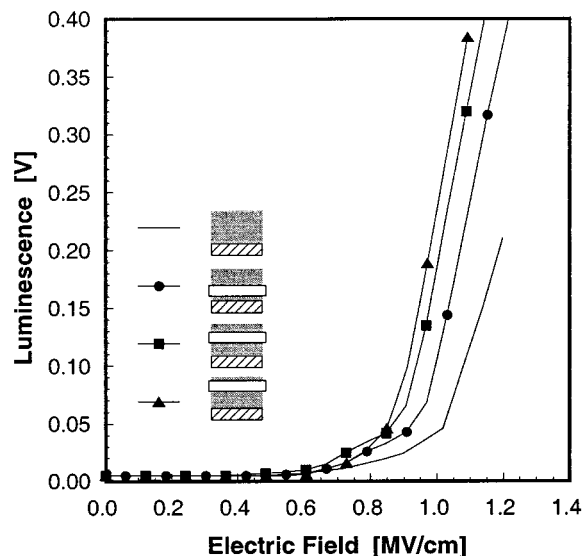


Figure 4. Luminescence versus electric field measurements. Luminescence is given in volts as a direct signal of the detector output (MLA-1, straight line; MLA-2, filled circles; MLA-3, filled squares; MLA-4, filled triangles).

position. This demonstrates that the observed emission originates from the PPV and not from the clay layer.

Effect of the Layer Position. The efficiency of the device is related to the position of the clay layer within the devices. We find that the highest efficiency is obtained if the layer is close to the anode (ITO). Efficiency is smallest (most likely due to quenching by the metal) but still 14 times higher than in films without montmorillonite, if the isolating layer is close to the cathode (Al). A likely explication may be that the position of the isolating layer directs the position of the recombination zone although the exact mechanism of the

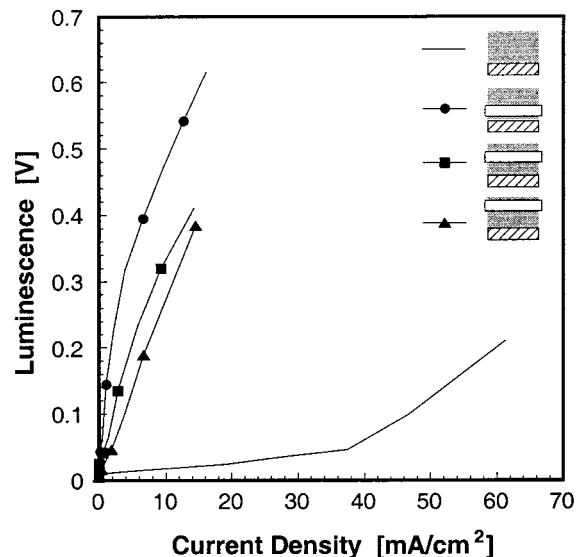


Figure 5. Luminescence-current density profiles showing the greatly enhanced performance of OLEDs containing a montmorillonite layer. The device without a clay layer (MLA-1, straight line) has a somewhat lower relative efficiency than those with an isolating layer. Device efficiency is further increased when the isolating inorganic layer is close to the ITO anode (MLA-2, filled circles).

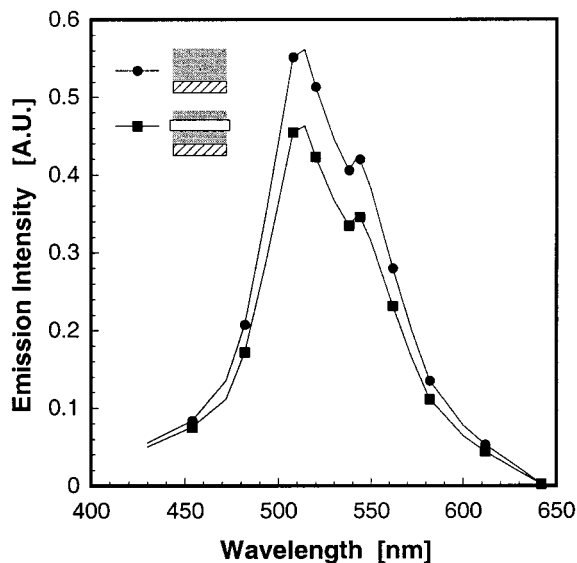


Figure 6. Emission spectra obtained from a device without clay layer (filled circles) and from a device containing a montmorillonite layer at position 10 (sample MLA-3, filled squares). Spectra from OLED devices with clay layers in different positions (data not shown) show the same characteristics as sample MLA-3, indicating that the observed emission arises from the PPV only and that the emission does not change much in the presence of the clay layer.

action of the inorganic layer is not yet known. First of all it is not known if the inorganic layer composed of individual clay platelets constitutes a perfect electrical barrier or if charge carriers are only “deflected” and “channeled” through the pores that might be present between different sheets. This would lead to a higher density of charge carriers passing in the small pore volume between the sheets and thus to a higher recombination probability in this region. This case is depicted in cartoon-like fashion in Figure 7 on the left. On the right

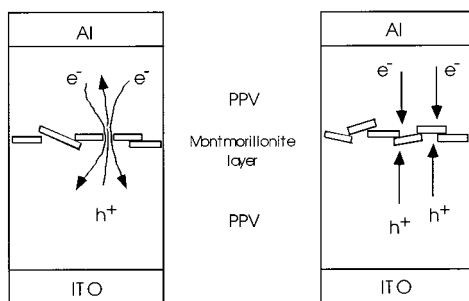


Figure 7. Simplified representation of charge transport in an electroluminescent device containing an “isolating” layer composed of individual montmorillonite platelets, e^- and h^+ represent electrons and holes, respectively. On the *left* carriers pass through pore defects, on the *right* carriers accumulate above and below the isolating layer.

of Figure 7 we depict the situation where charge carrier transport is hindered by the inorganic barrier, thus causing charge accumulation above and below the isolating layer in which electrons and predominantly holes form a so-called “space charge layer”.²⁸ In this case, one could expect an enhanced recombination probability for the carriers traversing the barrier layer, as they pass through the zone of accumulated carriers of the opposite sign (“space charge layer”).

We have clearly demonstrated the effect of introducing an isolating montmorillonite clay layer in the architecture of OLEDs composed of 20 layer pairs of PMA and the classic PPV: device performance increases by a factor of at least 14 in the presence of a barrier layer. Drastic enhancements of device efficiency are not uncommon and have for example been observed by fine-tuning the electrode film interface.³ At present we can only speculate about the mechanism responsible for the effects reported here. This concerns both the function of the barrier layer and its position within the device. It is clear that this will be difficult as a detailed structural characterization of the mineral layer is not an easy task and it will be necessary to rely to a large extent on variation of film architecture in conjunction with device characteristics. Especially the question if and how the clay layers influence the interfacial roughness needs to be addressed, but data are not yet available.

This is only a first report on the subject, in the future we are planning to investigate the observed effects of OLED architecture on device performance in more detail. However, we would like to point out that the layer-by-layer deposition technique is a powerful tool to very reproducibly fabricate OLEDs with active areas of over 1 cm² that are very homogeneous. Furthermore, one can easily put different materials (isolating oxide or conducting metal particles or even electroluminescent colloids) at different positions within

multilayer OLEDs, thus creating nonclassic devices with subnanometer precision.

Acknowledgment. We acknowledge support from the European Commission (contract HPRN-CT-2000-00003) from the European Associated Laboratory “Polymers in confined media” and from La Région Alsace (contract 96/928/03/623). We thank Sigurd Schrader (University of Potsdam, Germany) for helpful discussions.

References

- (1) Burroughes, J. H.; Bradley, D. D. C.; Marks, R. N.; Mackay, K.; Friend, R. H.; Burns, P. L.; Holmes, A. B. *Nature* **1990**, *347*, 539–541.
- (2) Brown, A. R.; Bradley, D. D. C.; Burroughes, J. H.; Friend, R. H.; Greenham, N. C.; Burn, P. L.; Holmes, A. B.; Kraft, A. *Appl. Phys. Lett.* **1992**, *61*, 2793–2795.
- (3) Ho, P. K. H.; Kim, J. S.; Burroughes, J. H.; Becker, H.; Li, S. F. Y.; Brown, T. M.; Cacialli, F.; Friend, R. H. *Nature* **2000**, *404*, 481–484.
- (4) Decher, G.; Hong, J.-D.; Schmitt, J. *Thin Solid Films* **1992**, *210/211*, 831–835.
- (5) Decher, G. *Science* **1997**, *277*, 1232–1237.
- (6) Fou, A. C.; Onitsuka, O.; Ferreira, M.; Rubner, M. F. *J. Appl. Phys.* **1996**, Vol. 79, 7501–7509.
- (7) Onitsuka, O.; Fou, A. C.; Ferreira, M.; Hsieh, B. R.; Rubner, M. F. *J. Appl. Phys.* **1996**, Vol. 80, 4067–4071.
- (8) Bliznyuk, V. R. B.; Brock, P. J.; Scherf, U.; Carter, S. A. *Adv. Mater.* **1999**, Vol. 11, 1257–1261.
- (9) Arango, A. C.; Carter, S. A.; Brock, P. J. *Appl. Phys. Lett.* **1999**, Vol. 74, 1698–1700.
- (10) Liu, Y.; Wang, A.; Claus, R. *J. Phys. Chem. B* **1997**, *101*, 1385–1388.
- (11) Liu, Y.; Wang, A.; Claus, R. *J. Chem. Phys. B* **1997**, *101*, 5273–5274.
- (12) Gao, M.; Richter, B.; Kirstein, S. *Adv. Mater.* **1997**, *9*, 802–805.
- (13) Hong, H.; Steitz, R.; Kirstein, S.; Davidov, D. *Adv. Mater.* **1998**, *119*, 1104–1107.
- (14) Kotov, N. A.; Haraszty, T.; Turi, L.; Geer, R. E.; Dekany, I.; Fendler, J. H. *J. Am. Chem. Soc.* **1997**, *119*, 6821–6832.
- (15) Kleinfeld, E. R.; Ferguson, G. S. *Science* **1994**, *265*, 370–373.
- (16) Kleinfeld, E. R.; Ferguson, G. S. *Chem. Mater.* **1995**, *7*, 2327–2335.
- (17) Lvov, Y.; Ariga, K.; Ichinose, I.; Kunitake, T. *Langmuir* **1996**, *12*, 3038–3044.
- (18) Struth, B.; Eckle, M.; Decher, G.; Oeser, R.; Simon, P.; Schubert, D. W.; Schmitt, J. *Europ. Phys. J. E—Soft Matter*, submitted for publication.
- (19) Giannelis, E. P. *Adv. Mater.* **1996**, *8*, 29–35.
- (20) Krishnamoorti, R.; Viai, R. A.; Giannelis, E. P. *Chem. Mater.* **1996**, Vol. 8, 1728–1734.
- (21) Pinnavaia, T. J.; Lan, T.; Wang, Z.; Shi, H.; Kaviratna, P. D. *Nanotechnology* **1996**, 250–261.
- (22) Ijdo, W. L.; Lee, T. J.; Pinnavaia, T. J. *Adv. Mater.* **1996**, *8*, 79–83.
- (23) Grüner, J.; Remmers, M.; Neher, D. *Adv. Mater.* **1997**, *9*, 964–968.
- (24) Wessling, R. A. *J. Polym. Sci.: Polym. Symp.* **1985**, *72*, 55–66.
- (25) Gagnon, D. R.; Capistran, J. D.; Karasz, F. E.; Lenz, R. W.; Antoun, S. *Polymer* **1987**, *28*, 567–573.
- (26) Lenz, R. W.; Han, C. C.; Stenger-Smith, J.; Karasz, F. E. *J. Polym. Sci.: Part A: Polym. Chem. Ed.* **1988**, *26*, 3241–3249.
- (27) Kern, W. *Semiconductor Int.* **1984**, 94–99.
- (28) See for example: Deussen, M and Bäessler, H. *Chemie in unserer Zeit* **1997**, *2*, 76–86.

NL005514A